AIP Journal of Applied Physics

Role of magnesium in band gap engineering of sub-monolayer type-II ZnTe quantum dots embedded in ZnSe

Qiang Zhang, Aidong Shen, Igor L. Kuskovsky, and Maria C. Tamargo

Citation: J. Appl. Phys. **110**, 034302 (2011); doi: 10.1063/1.3611418
View online: http://dx.doi.org/10.1063/1.3611418
View Table of Contents: http://jap.aip.org/resource/1/JAPIAU/v110/i3
Published by the American Institute of Physics.

Additional information on J. Appl. Phys.

Journal Homepage: http://jap.aip.org/
Journal Information: http://jap.aip.org/about/about_the_journal
Top downloads: http://jap.aip.org/features/most_downloaded
Information for Authors: http://jap.aip.org/authors

ADVERTISEMENT

Downloaded 18 Jun 2013 to 149.4.205.28. This article is copyrighted as indicated in the abstract. Reuse of AIP content is subject to the terms at: http://jap.aip.org/about/rights_and_permissions

JOURNAL OF APPLIED PHYSICS **110**, 034302 (2011)

Role of magnesium in band gap engineering of sub-monolayer type-II ZnTe quantum dots embedded in ZnSe

Qiang Zhang,[1,a)] Aidong Shen,[2] Igor L. Kuskovsky,[3] and Maria C. Tamargo[4]
[1]*Department of Physics, The City College of CUNY, New York, New York 10031, USA*
[2]*Department of Electrical Engineering, The City College of CUNY, New York, New York 10031, USA*
[3]*Department of Physics, Queens College of CUNY, Queens, New York, 11367, USA*
[4]*Department of Chemistry, The City College of CUNY, New York, New York 10031, USA*

(Received 10 February 2011; accepted 17 June 2011; published online 1 August 2011)

Modification of the bandgap of sub-monolayer type-II ZnTe quantum dots (QDs), by means of direct incorporation of magnesium in the QDs, is reported. Nitrogen co-doped QDs embedded in a ZnSe matrix have been grown by a migration-enhanced molecular beam epitaxy technique. Incorporation of Mg in the ZnTe QDs decreases the valence band discontinuity, leading to reduced localization of the holes, which results in a higher electrical conductivity in the samples as deduced from the Hall effect measurements. The type-II alignment of the bands in the QDs is supported by intensity dependent and time-resolved photoluminescence measurements. Hall effect measurements indicate that the material has p-type conductivity with mid-10^{15} carriers/cm^3 and hole mobilities in the 5–50 cm^2/V·s range. © *2011 American Institute of Physics*. [doi:10.1063/1.3611418]

I. INTRODUCTION

There is an increasing interest in type-II quantum structures due to their tunable optical and electrical properties by taking advantage of the type-II band alignment and quantum confinement effects.[1] Among them, type-II ZnTe/ZnSe quantum dots (QDs) are particularly interesting because of their relatively large valence band and conduction band offsets.[2] Furthermore, II–VI wide bandgap semiconductors, such as ZnSe, have long been difficult to dope p-type. This difficulty still constitutes a problem for practical uses of these materials, non-withstanding the promise of such a material in light emitters in the blue-green spectral region. More generally, the successful bipolar doping of wide bandgap semiconductors is still a subject of great interest, and the composite material system containing QDs may be a viable solution to such a problem.

This doping hurdle resides in obtaining adequate dopant incorporation in the material, which is limited by poor solubility and/or excessive compensation.[3] In the case of ZnSe, it is relatively easy to obtain n-type doping, while in ZnTe, p-type doping is more readily obtained.[4] Many studies on both bulk and epitaxial layers have been carried out to address this problem. Previously, a high net acceptor concentration of 6×10^{18} cm^{-3} was achieved for ZnSe by the migration enhanced molecular beam epitaxy (ME-MBE) technique, incorporating N within ZnTe nanoclusters embedded in the ZnSe, while keeping relatively low overall content of Te.[5,6] Unfortunately, this material exhibits rather low free hole concentrations, so that although high net acceptor concentrations were achieved, the conductivity of the layers remained low. We attribute this low conductivity to the localization of the holes in the valence band wells produced by the type II QDs because of from the large valence band discontinuity (~0.7 eV) between ZnTe and ZnSe.[7]

To modify the band structure and reduce the localization of the holes, with the purpose of achieving a higher conductivity of the samples, a series of samples with added Mg in the ZnTe QDs have been grown by ME-MBE. The x-ray diffraction (XRD) measurements confirm the incorporation of Mg in the samples, while reflectance spectrum data suggest that there is no significant Mg incorporation within ZnSe barriers, i.e., Mg is confined to the ZnTe QD regions. The type-II nature of the Mg containing ZnTe QDs is confirmed by cw intensity-dependent and time-resolved photoluminescence (PL) studies. Furthermore, we have been able to perform the Hall effect measurement on the N-doped type-II QD samples, which is not possible in samples without Mg, indicating that the modified band structure has reduced the confinement of the holes resulting in increased layer conductivity.

II. EXPERIMENTAL

All the samples were grown on (100) GaAs substrates in a Riber 2300 MBE system, which contains a III–V chamber and a II–VI chamber connected by ultrahigh vacuum (UHV), following procedures previously used to grow ZnTe/ZnSe type-II QDs.[8] Oxide desorption of the GaAs substrates was performed in the III–V chamber by heating the substrates to ~580 °C under an As flux, after which a 100 nm GaAs buffer layer was grown with a streaky (2×4) reflection high-energy electron diffraction (RHEED) surface pattern. The substrate with the GaAs buffer layer was transferred to the II–VI chamber under UHV. To avoid the formation of Ga_2Se_3 at the III-V/II-VI interface, which is expected to result in the formation of stacking faults, we exposed the sample to a Zn-flux before the growth of a 5 nm ZnSe buffer layer at 200 °C. Then a 50 nm undoped ZnSe buffer layer was grown at 300 °C under Se rich conditions with a growth rate of ~0.3 μm/h. A streaky (2×1) RHEED pattern was observed after the buffer layer growth. The buffer layer was followed by the ME-MBE growth cycles leading to the type II nanoislands embedded in ZnSe.

[a)]Electronic mail: ccnyqzhang@gmail.com.

 © 2011 American Institute of Physics

Downloaded 18 Jun 2013 to 149.4.205.28. This article is copyrighted as indicated in the abstract. Reuse of AIP content is subject to the terms at: http://jap.aip.org/about/rights_and_permissions

Three cycles of shutter operations were employed to carry out the ME-MBE. In cycle 1, right after the ZnSe growth, the Se shutter was closed. Then there was a 5 s growth interruption to desorb the excess Zn from the surface, and then the Te shutter was opened to deposit Te on the Zn-terminated surface for 5 s and followed by another 5 s growth interruption. Cycle 2 was almost identical to cycle 1 except that instead of the exposure of the surface to Zn, we either opened the Mg shutter only (exposed the surface only to Mg) or opened the Zn and Mg shutters simultaneously. This was followed by cycle 3, which was identical to cycle 1. The Zn shutter was opened for 5 s after cycle 3, and then another ZnSe spacer was grown before repeating the entire sequence 100 or 200 times. This shutter operations produce the sequential deposition of the elements, which, combined with the short interruptions, give rise to enhanced surface migration and the formation of self-assembled Zn(Mg)Te QDs.[1,9,10]

The sample crystalline quality and the Mg content were assessed by (400) XRD rocking curves using a Cu $K\alpha_1$ radiation. Low temperature and temperature-dependent PL measurements were carried out using a closed cycle refrigeration system. The 351 nm emission line from an Argon ion laser was used as the excitation source, and the excitation intensity was varied with the aid of neutral density filters. A semiconductor laser with a pulse duration of the order of a nanosecond was employed in the time-resolved PL measurements.

III. RESULTS AND DISCUSSION

As shown in Table I, two sets of samples were grown. In set 1, both were grown with Zn and Mg co-deposition during the central ME-MBE cycle (cycle 2). However, the temperature of the Mg source is 20 °C higher in A2 than in A1. By contrast, the samples in set 2 were grown with only Mg deposition in cycle 2. The last sample (B3) in set 2 was grown with an intermediate Mg temperature (210 °C) and an intentionally greater total thickness (200 repeats) to allow performing the Hall effect measurement.

First, the controllable Mg incorporation is confirmed by the XRD rocking curve measurements, shown in Fig. 1. For each sample, the sharp peak with the highest intensity represents the (400) reflection of the GaAs substrate, and the broad peak with relatively low intensity represents the zero-order satellite peak of the periodic structure, which is located at the small-angle side of the GaAs peak due to the larger lattice constants of the ZnSe (5.67 Å), ZnTe (6.10 Å), and MgTe (6.37 Å) relative to GaAs (5.65 Å). The zero-order satellite peaks are broadened, due to the lattice-mismatch between the II–VI epitaxial layers and the GaAs substrate, and period dispersion.[11,12] In the inset of Fig. 1, the shift between the zero-order satellite peak and the GaAs substrate peak is plotted as a function of the Mg source temperature, listed in Table I. Samples of same thickness with higher Mg source temperature show larger shifts than those with lower Mg temperature, indicating higher average Mg content. Furthermore, there is a greater effect on the change of the lattice constants when there is only Mg incorporated in the middle of the deposition, suggesting a higher average concentration of Mg in the ZnTe/ZnSe type-II QDs by this approach. The shift of the thicker sample B3 does not line up with the shifts of B1 and B2, which is most likely due to the partial relaxation of this thicker layer, also consistent with somewhat broader XRD zero-order satellite peak of B3. To rule out incorporation of Mg in the ZnSe barrier region, we performed reflectance measurements of our samples. An absorption edge at 2.7 eV, as expected for pure ZnSe, was measured for the samples, suggesting that the Mg was incorporated largely within the QDs themselves.

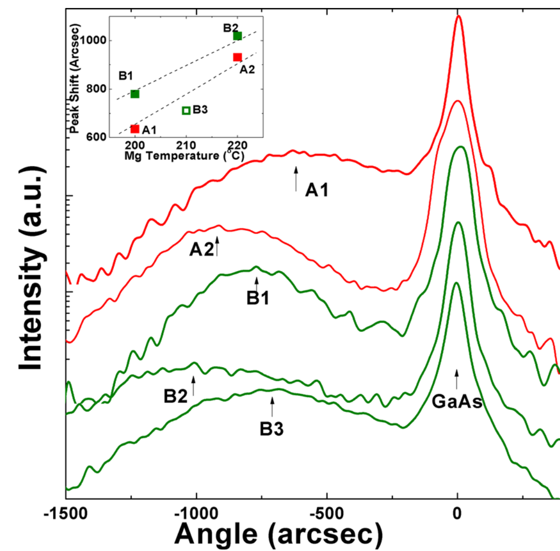

FIG. 1. (Color online) The (400) XRD rocking curve spectra for the samples with different Mg incorporation. The broad peak represents the zero-order satellite peak of the multiple QD layer for each sample. Inset shows the peak shift of each sample as a function of Mg growth temperature. Dashed lines in the inset are drawn for eye.

The samples were characterized by cw intensity dependent PL measurements, shown in Fig. 2 for sample B3. In the inset, the PL peak position is plotted as a function of relative excitation intensity. A significant blueshift with increasing excitation intensity (plotted in the inset) was observed, illustrating the band bending effect due to the type-II band

TABLE I. Two sets of ZnTe/ZnSe QDs samples.

Sample		T_{Mg} (°C)	No. of repeats	ZnSe spacer	Cycle 1		Cycle 2			Cycle 3	
Set 1	A1	200	100	5.7nm	Zn	(Te + N)	(Zn + Mg)	(Te + N)	Zn	(Te + N)	Zn
	A2	220	100	5.7nm	Zn	(Te + N)	(Zn + Mg)	(Te + N)	Zn	(Te + N)	Zn
Set 2	B1	200	100	5.7nm	Zn	(Te + N)	Mg	(Te + N)	Zn	(Te + N)	Zn
	B2	220	100	5.7nm	Zn	(Te + N)	Mg	(Te + N)	Zn	(Te + N)	Zn
	B3	210	200	5.7nm	Zn	(Te + N)	Mg	(Te + N)	Zn	(Te + N)	Zn

Downloaded 18 Jun 2013 to 149.4.205.28. This article is copyrighted as indicated in the abstract. Reuse of AIP content is subject to the terms at: http://jap.aip.org/about/rights_and_permissions

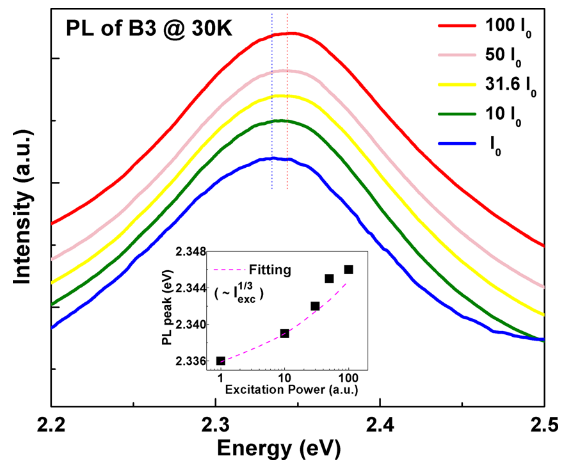

FIG. 2. (Color online) The PL spectra of B3 at 30 K with different excitation intensity (I_{exc}). The peak position is plotted as a function of I_{exc} in the inset, and the dashed line is the fitting curve, following the cube root dependence of I_{exc}.

alignment (e.g., Refs. 13 and 14, and references therein) between the QDs and the ZnSe matrix. The dashed line in the inset is the fitting curve, following a cube root dependence of the excitation intensity, a particular property of the type-II heterostructures.[15] Note that compared with Ref. 1, the PL intensity dependence is observed in fewer orders of magnitude. This could be related to the significantly lower overall PL intensity of the doped samples due to strong non-radiative contribution,[16] similarly to that reported for nitrogen doped ZnTe/ZnSe system.

The existence of type-II QDs is further supported by the time-resolved PL measurements shown in Fig. 3. The PL decay curves cannot be fitted by a single exponential, reflecting the dependence of the decay time on the concentration of photogenerated carriers.[9] We thus used a biexponential fitting to extract the decay times, following the procedure of Ref. 9. The extracted decay times τ_1 and τ_2 are plotted as a function of temperature in inset (a). The fast decay time τ_1 can be treated as a combination of fast decay in type-II QDs due to increased overlap of the electron and hole wavefunctions and the intrinsic lifetimes for the bulk ZnSeTe alloy[9]; the slow decay time τ_2 can thus be treated as intrinsic to type-II QDs (the so-called "flatband condition")[9]. A careful study of the data shows that τ_2 remains almost constant in the temperature range of 30 to 80 K. It then decreases quickly in the temperature range of 80 to 160 K to the values that cannot be resolved in our set-up. This behavior is understood by the following reasoning.

In these type-II QDs, holes are relatively strongly confined within the dots, whereas the electrons are weakly bound to the holes via the Coulomb interaction. The first temperature interval is characterized by the ionization of weakly bound electrons, which should decrease the overall lifetime; however, this process is compensated by the fact that the electrons can be recaptured at the QDs, increasing the observed lifetime.[9] The competition between these two mechanisms is responsible for the observed nearly constant lifetime as reported in other type-II QDs due to the common property of well-localized zero-dimensional carriers.[13,17] Moreover, we point out that there is a small increase in the lifetime from 30 to 50 K; this is similar to that observed in Ref. 9, further supporting our conclusion about type-II nature of the grown QDs. With further increase of the temperature, a non-radiative mechanism responsible for hole ionization becomes dominant, evident by the fact that the PL intensity simultaneously decreases in that temperature range, as shown in inset (b).[9] We plot inverse of the lifetime τ_2 versus inverse temperature (in units of energy) in Fig. 4, which we fit to estimate the hole ionization energy E_A. The obtained value is ~82 meV. This is a reasonable value when compared with the reported activation energies for nitrogen in ZnTe (e.g., 51 meV in ZnTe-ZnSe SL (Ref. 18); 46 meV (Ref. 19) to 53 meV (Ref. 20) to 57 meV (Ref. 21) in bulk ZnTe, depending on the doping levels), because, due to the QD confinements and larger band gaps in ZnMgTe, one should expect a higher ionization energy. The same fitting gives the radiative decay lifetime of ~28 ns, which is much shorter than that reported in Ref. 1. We again attribute this to the doping.[16]

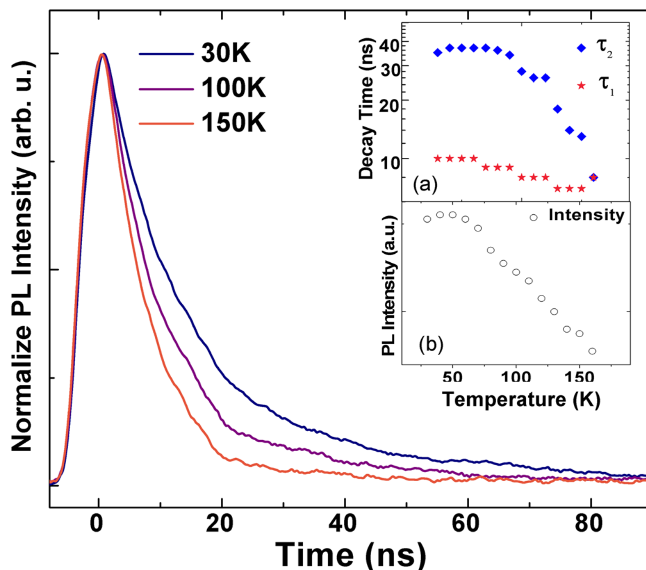

FIG. 3. (Color online) The time-resolved PL spectra of sample B3 at different temperatures. The lifetimes τ_1 and τ_2 are plotted as a function of temperature in inset (a). The PL intensity is plotted as a function of temperature in inset (b).

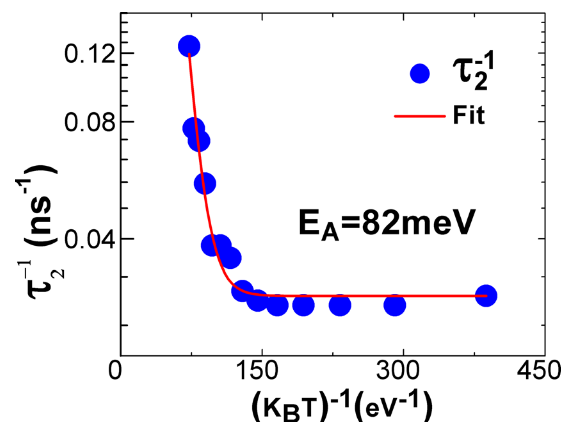

FIG. 4. (Color online) The inverse of the lifetime τ_2 is plotted as a function of inverse temperature (in the units of energy), leading to the hole ionization energy $E_A = 82$ meV.

Downloaded 18 Jun 2013 to 149.4.205.28. This article is copyrighted as indicated in the abstract. Reuse of AIP content is subject to the terms at: http://jap.aip.org/about/rights_and_permissions

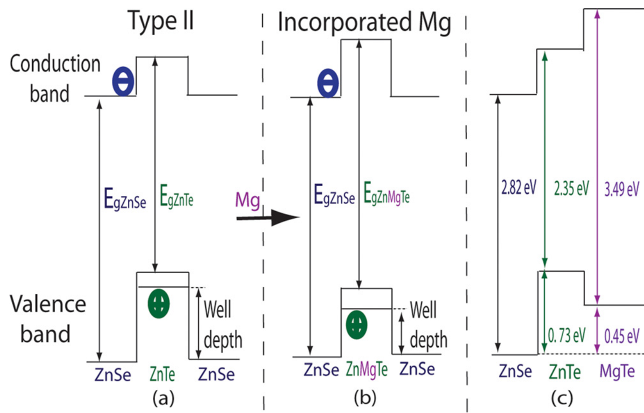

FIG. 5. (Color online) (a) Schematic of the type II band structure for ZnTe QDs in ZnSe. (b) Modified band structure by incorporating Mg in the QDs. (c) Predicted band alignments for ZnSe, ZnTe and MgTe.

The Mg incorporation within QDs should modify the valence band alignment in such a way that the hole confinement in the QDs is reduced, which increases the probability of hole delocalization and greater conductivity. The expected modified band structure of the type II QDs when the Mg is incorporated within the ZnTe is schematically shown in Fig. 5, along with the predicted band alignments for ZnSe, ZnTe, and MgTe.[22,23] One may assume that the valence band maximum of the chalcogenides is a linear function of composition, hence one can estimate the band offset between chalcogenides of different composition.[22] For example, an incorporation of 32% Mg in ZnTe could induce a 90 meV reduction of the valence band offset between ZnTe and ZnSe. With a smaller valence band offset, the confinement of the holes is reduced, and they may be more easily activated for conductivity. The addition of Mg in the QDs may also affect the growth morphology of the QDs, possibly changing their size and/or shape. Further work is needed to fully assess these factors. However, the basic findings reported here, i.e., the reduced hole confinement in the samples grown with Mg incorporation, should remain valid.

Prior attempts to perform Hall effect measurements on samples of N-doped ZnTe nano-islands in ZnSe were not

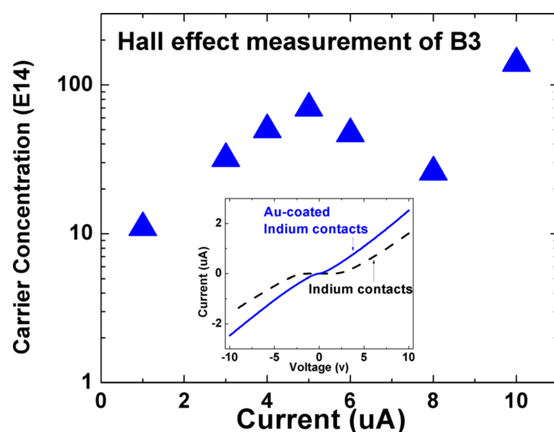

FIG. 6. (Color online) Hall effect result varies with the current we applied to the sample, possibly resulting from the metal-semiconductor contacts. The inset shows the ohmic characteristics of the Au contacts.

successful even when high net acceptor concentrations were measured by C-V techniques.[5] Sample B3 was prepared with Au contacts in the corners according to the Van-der Pauw technique.[24] As shown in the inset in Fig. 6, the Au contacts show nearly ohmic *I-V* characteristics. Hall effect measurements of sample B3 give p-type conductivity with hole concentrations in the range of mid 10^{15} cm^{-3}, and the hole mobilities in the range of 5–25 cm^2/V·s. Although the carrier concentration achieved here is rather low, the results clearly suggest successful reduction of the valence band offset between ZnSe barriers and ZnMgTe QDs compared to the ZnTe/ZnSe QD system.

IV. CONCLUSIONS

In conclusion, we have grown type-II ZnTe/ZnSe QDs by a ME-MBE process, with Mg incorporated at various levels during the ME-MBE process, to adjust the type-II QD band structure and reduce the localization of the holes. XRD measurements show controllable Mg incorporation. Intensity dependent and time-resolved PL measurements confirm the type-II band alignment of the QDs. We propose that the incorporation of Mg reduces the confinement of the holes, which is furthermore supported by the ability to perform Hall effect measurements. These results illustrate the potential of band structure engineering of type II nanostructures to enhance materials properties.

ACKNOWLEDGMENTS

The authors gratefully acknowledge Dr. Bingsheng Li for sample preparation and helpful discussions. This work was supported by Department of Energy grant number DE-FG02-10ER46678.

[1]Y. Gong, W. MacDonal, G. F. Neumark, M. C. Tamargo, and I. L. Kuskovsky, Phys. Rev. B **77**, 155314 (2008).
[2]F. Malonga, D. Bertho, C. Jouanin, and J. M. Jancu, Phys. Rev. B **52**, 5124 (1995).
[3]G. F. Neumark, R. M. Park, and J. M. Depuydt, Phys. Today **47**(6), 26 (1994).
[4]D. J. Chadi, Phys. Rev. B **59**, 15181 (1999).
[5]W. Lin, S. P. Guo, M. C. Tamargo, I. Kuskovsky, C. Tian, and G. F. Neumark, Appl. Phys. Lett. **76**, 2205 (2000).
[6]I. L. Kuskovsky, Y. Gu, Y. Gong, H. F. Yan, J. Lau, I. C. Noyan, G. F. Neumark, O. Maksimov, X. Zhou, M. C. Tamargo, V. Volkov, Y. Zhu, and L. Wang, Phys. Rev. B **73**, 195306 (2006).
[7]S.-H. Wei and A. Zunger, Appl. Phys. Lett. **72**, 2011 (1998).
[8]I. L. Kuskovsky, C. Tian, G. F. Neumark, J. E. Spanier, I. P. Herman, W. C. Lin, S. P. Guo, and M. C. Tamargo, Phys. Rev. B **63**, 155205 (2001).
[9]Y. Gu, I. L. Kuskovsky, M. Voort, G. F. Neumark, X. Zhou, and M. C. Tamargo, Phys. Rev. B **71**, 045340 (2005).
[10]I. L. Kuskovsky, Y. Gong, G. F. Neumark, and M. C. Tamargo, Superlattices Microstruct. **47**, 87 (2010).
[11]D. K. Bowen and B. K. Tanner, *High Resolution X-ray Diffractometry and Topography* (Taylor and Francis, 1998), Chap. 6.
[12]Y. Gong, H. F. Yan, I. L. Kuskovsky, Y. Gu, I. C. Noyan, C. F. Neumark, and M. C. Tamargo, J. Appl. Phys. **99**, 064913 (2006).
[13]F. Hatami, M. Grundmann, N. N. Ledentsov, F. Heinrichsdorff, R. Heitz, J. Bohrer, D. Bimberg, S. S. Ruvmov, P. Werner, V. M. Ustinov, P. S. Kop'ev, and Zh. I. Alferov, Phys. Rev. B **57**, 4635 (1998).
[14]Y. Gu, I. L. Kuskovsky, M. van der Voort, G. F. Neumark, X. Zhou, and M. C. Tamargo, Phys. Rev. B **71**, 045340 (2005).
[15]T. T. Chen, C. L. Cheng, Y. F. Chen, F. Y. Chang, H. H. Lin, C.-T. Wu, and C.-H. Chen, Phys. Rev. B **75**, 033310 (2007).

Downloaded 18 Jun 2013 to 149.4.205.28. This article is copyrighted as indicated in the abstract. Reuse of AIP content is subject to the terms at: http://jap.aip.org/about/rights_and_permissions

[16]I. L. Kuskovsky, C. Tian, C. Sudbrack, G. F. Neumark, W. C. Lin, P. Guo, and M. C. Tamargo, J. Appl. Phys. **90**, 2269 (2001).
[17]C. H. Wang, T. T. Chen, Y. F. Chen, M. L. Ho, C. W. Lai, and P. T. Chou, Nanotechnology **19**, 115702 (2008).
[18]S. Sakakibara, N. Amano, K. Ishino, A. Ishida, and H. Fujiyasu, Jpn. J. Appl. Phys. **32**, 4703 (1993).
[19]Y. Fan, J. Han, L. He, J. Saraie, R. L. Gunshor, M. Hagerott, and A. V. Nurmikko, J. Electron. Mater **23**, 245 (1994).
[20]T. Baron, K. Saminadayar, and N. Magnea, J. Appl. Phys. **83**, 1354 (1998).
[21]P. J. Dean, H. Venghaus, J. C. Pfister, B. Schaub, and J. Marine, J. Lumin. **16**, 363 (1978).
[22]S. Wei and A. Zunger, J. Appl. Phys. **78**(6), 3846 (1995).
[23]O. M. Madelung, *Semiconductors: Data Handbook*, 3rd ed. (Springer, Berlin, 2004).
[24]L. J. van der Pauw, Philips Res. Rep. **13**, 1 (1958).

Downloaded 18 Jun 2013 to 149.4.205.28. This article is copyrighted as indicated in the abstract. Reuse of AIP content is subject to the terms at: http://jap.aip.org/about/rights_and_permissions